A Porous Iron Electrode for Electrochemical Ammonia Synthesis

Joost P.J. Olsthoorn

Master Thesis
Materials for Energy Conversion and Storage (MECS)
Department of Chemical Engineering
Faculty of Applied Sciences

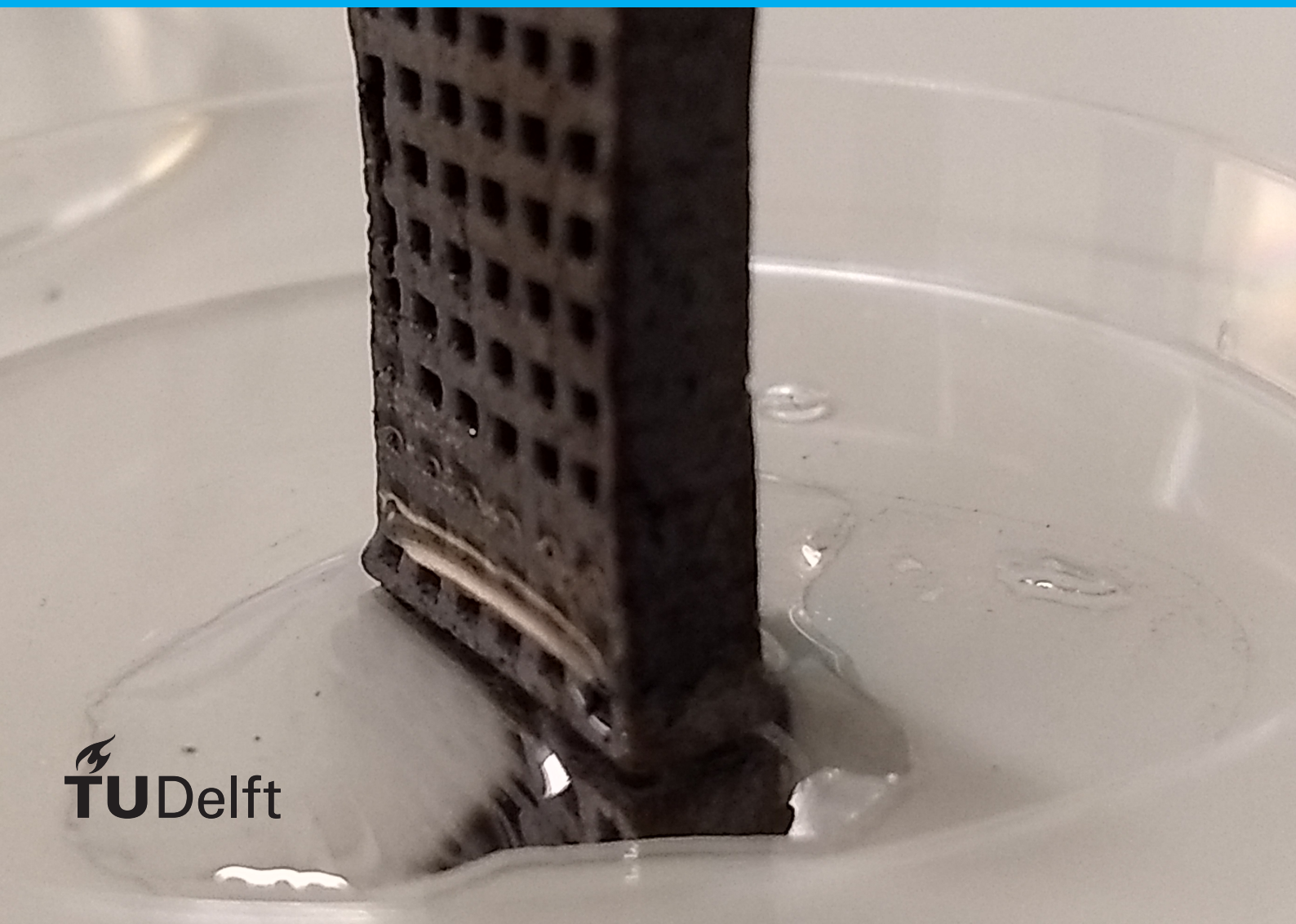

TU Delft

A Porous Iron Electrode for Electrochemical Ammonia Synthesis

by

Joost P.J. Olsthoorn

to obtain the degree of Master of Science in Sustainable Energy Technology
at the Delft University of Technology,
to be defended publicly on Wednesday March 13th, 2024 at 10:45 AM.

Student number: 4150384
Project duration: November 28, 2022 – March 13, 2024
Thesis committee:

Prof. dr. F.M. Mulder,	TU Delft, MECS group, project supervisor
Prof. dr. A. Urakawa,	TU Delft, Catalysis Engineering
Dr. R. Kortlever,	TU Delft, Process & Energy, Large Scale Energy Storage
M.P. Jungbacker,	TU Delft, MECS group, daily supervisor

TU Delft

Abstract

Ammonia is a precursor in fertilizer production and a potential carbon-free energy carrier, which is essential for the energy transition to more renewable energy sources. To that end, the current fossil fuel based method of industrial ammonia production through the Haber-Bosch process should be replaced by electrochemical ammonia synthesis. However, research into this topic faces several challenges, including a strong dinitrogen bond, competition from the hydrogen evolution reaction and low solubility of nitrogen in aqueous electrolytes, limiting the availability of nitrogen at the reaction sites on the electrode surface. In this study, in order to better understand these limitations to electrochemical nitrogen reduction to ammonia, a porous iron electrode is used in a cell design allowing both aqueous electrolyte and nitrogen gas access to the surface, which is successfully reduced electrochemically to serve as a nitrogen dissociation catalyst. Careful control of the applied potential limits the competition from the hydrogen evolution reaction. Nuclear magnetic resonance spectroscopy and ion chromatography measurements of the electrolyte were performed to check for possible contamination by nitrogen containing species. Small amounts of ammonia were measured using gas chromatography-mass spectroscopy on the gas output, but only with a high residence time of the nitrogen gas inside the cell. Since reduced iron surfaces are known to be good nitrogen dissociation catalysts, even at ambient temperature and pressure, the cause of the low ammonia production rate reported here is the abundant presence of water, which blocks nitrogen from the surface adsorption sites even when the catalytic surface is not submerged in the electrolyte. These results show that creating a surface with sufficient catalytic activity to break the dinitrogen bond is very well possible, but the main challenge is keeping the surface clean to prevent blocking of the reaction sites. This gives additional insight for future efforts in developing electrochemical ammonia synthesis methods.

Contents

1 Introduction

While the negative effects of global anthropogenic climate change are becoming increasingly clear, the European Union is promoting an expansion of renewable wind and solar energy as part of the Green New Deal in order to combat climate change by reducing CO_2 emissions.[1] These new energy sources produce electricity intermittently according to natural variations of sun and wind, resulting in a mismatch between supply and demand on the electricity grid. This mismatch shows a need for both seasonal and daily energy storage.[2] Current capacity for energy storage is already insufficient to deal with intermittency from renewable energy sources, as shown by negative electricity prices becoming more common during hours of peak renewable energy production.[3] Batteries are an excellent short-term energy storage solution, due to their high efficiency. However long-term energy storage in batteries is undesirable due to their slow self-discharge. Therefore, artificial fuels are more suitable for long-term energy storage. Additionally, these artificial fuels can be used to decarbonise industries that are difficult to transition to renewable electricity. In the Green New Deal, the focus is on hydrogen for this purpose, however there are other options.

One of the more promising alternatives is ammonia. It is already widely used in industry, mostly as a precursor in fertilizer production. In fact, the process to synthesize ammonia from its elements, nitrogen and hydrogen, was first developed by Fritz Haber and Carl Bosch and can be considered one of the greatest inventions of the twentieth century, because it is responsible for sustaining the worldwide exponential population growth by allowing the large scale production of fertilizers for agriculture.[4,5] The ammonia synthesis from nitrogen and hydrogen can be represented as follows:

$$N_2 + 3\,H_2 \longrightarrow 2\,NH_3$$

The Haber-Bosch process is still the current state-of-the-art in commercial ammonia production, however it is very energy intensive and emits carbon-dioxide.[6] It is responsible for 1-2% of global energy consumption[7] and about 1.4% of global CO_2 emissions.[8] A more sustainable ammonia production process is therefore of interest.

Producing ammonia electrochemically using renewable electricity can allow for the use of ammonia as an energy carrier for storage of intermittently available renewable electricity as well as making the ammonia production process more sustainable. Ammonia can even solve several of the limitations and challenges of hydrogen as an energy carrier.[7] Ammonia is easier to liquefy than hydrogen, only needing 10 bar at room temperature or -33 °C at atmospheric pressure[8], where hydrogen would need 700 bar at room temperature[9] or -253 °C at atmospheric pressure.[10] Ammonia also has a higher volumetric energy density than hydrogen.[11]

However, research into electrochemical ammonia production has identified several challenges. First is the very stable bond and lack of dipole moment of the dinitrogen molecule N_2, which makes it mostly inert.[5] Breaking this bond requires a suitable catalyst.[6] Iron is commonly used for this purpose in the Haber-Bosch process and can also be used as electrode material in electrochemical ammonia production.[12] Nitrogen dissociation and reduction can then occur on the surface of this electrode at negative potential.

A second challenge occurs when using an aqueous electrolyte as the hydrogen source. The hydrogen evolution reaction, part of water electrolysis, will prevail over nitrogen adsorption and reduction on the electrode surface at negative potential. Adsorbed hydrogen atoms then form hydrogen gas, rather than being available for nitrogen hydrogenation.[5] Other challenges include blocking of the nitrogen adsorption sites by the electrolyte, containing water and other species which can adsorb, and the rather poor solubility of nitrogen in an aqueous electrolyte, limiting the availability of nitrogen at the electrode surface. Finally, when producing ammonia in this way, it is obtained as a gas and partially dissolves in the electrolyte, therefore requiring a product separation step.[5]

Previous research at the MECS group has tackled these challenges by using a hydrogen permeation electrode, made from Ni instead of Fe, to separate a gas and liquid chamber, effectively separating the hydrogen evolution reaction (HER) and nitrogen reduction reaction (NRR) on both sides of the electrode.[5,13] Hydrogen is produced at the aqueous electrolyte side and permeates through the electrode to the nitrogen gas side as atomic hydrogen, where it reacts with adsorbed nitrogen to produce gaseous ammonia. This appeared to be possible with Ni, while Fe showed several challenges related to the Fe remaining oxidised which incapacitated hydrogen permeation and also prevented N_2 activation.

The purpose of this research is to investigate the use of a porous iron electrode in a setup where liquid and gas are separate, but where the liquid electrolyte can form a film on the electrode surface. This will make Fe reduction possible and the film is thin enough that N_2 still has access to the electrode surface. The combination of a reduced iron surface in contact with N_2 and a source of protons and electrons will allow for ammonia synthesis. Furthermore, the increased catalytic surface area is expected to increase the ammonia yield. The porous iron electrode is derived from previous research in the MECS group on a similar electrode for use in the battolyser, where reduction of Fe and reduced hydrogen production can be controlled.[14] However, one aspect that cannot be circumvented in this approach is the access of electrolyte to the iron surface. The research in this way aims to disentangle the limiting factors for Fe as a NRR catalyst further. The electrode will then be tested for the production of ammonia using the gas output of the aforementioned setup and performing gas chromatography coupled with mass spectrometry using a previously developed methodology.[15,16]

2

Theory

Making a porous iron electrode and using it for ammonia synthesis, requires several experimental steps. This chapter will explain the Haber-Bosch process, which is to be replaced by electrochemical ammonia synthesis, followed by the theoretical background of the catalysts used in ammonia synthesis. There will also be an explanation of the challenges in electrochemical ammonia synthesis and the work already done in the MECS group on this topic, which serves as a starting point for this research. This chapter will then discuss the theoretical background of the experimental methods employed and why a porous iron electrode should be capable of ammonia synthesis under the applied experimental conditions.

2.1. The Haber-Bosch process

While the Haber-Bosch process refers to a catalytic process for ammonia synthesis from hydrogen and nitrogen, in practice the process is preceded by nitrogen separation from the air and hydrogen production via steam methane reforming from natural gas. The latter process happens under high temperature and pressure and follows a two step reaction:[17]

$$CH_4 + H_2O \longrightarrow CO + 3\,H_2$$
$$CO + H_2O \longrightarrow CO_2 + H_2$$

The CO_2 is subsequently filtered out to obtain pure hydrogen gas. Steam methane reforming is responsible for over 80% of CO_2-emissions from the Haber-Bosch process.[18] Therefore, replacing the hydrogen source is often considered to be the first step in making the process more sustainable. Water electrolyzers powered by renewable electricity have already been used for this purpose in practice on a limited scale.[8]

After pure hydrogen and nitrogen gas are obtained, a mixture of these gasses is used for ammonia synthesis, which is a reversible exothermic reaction:[19]

$$N_2 + 3\,H_2 \longleftrightarrow 2\,NH_3$$

Although this reaction is exothermic, it has a high activation barrier since the dissociation of the nitrogen molecule is considered a very arduous process due to its strong triple bond energy of 941 kJ/mol.[5,19] Therefore, the reaction does not proceed spontaneously and there are some specific reaction conditions. These include a catalyst, usually solid iron or ruthenium particles, that can weaken the nitrogen molecule triple bond.[12,19] Also, following Le Chatelier's principle, a lower temperature will favor the forward reaction, since it is exothermic. However this will also lower the reaction rate. Therefore, since a high temperature is also needed to provide the necessary activation energy, the temperature in the reactor is at least 400 °C. Following the same principle, this high temperature must then be combined with a high pressure of around 200 bar to favor the forward reaction, where 4 mol of reactants form 2 mol of product.[19,20]

Fully replacing the Haber-Bosch process by electrochemical means provides even more benefits than just replacing steam methane reforming. This includes greater adaptability to the intermittency of renewable electricity sources, because an electrochemical process at near ambient temperature and pressure allows for much faster up- and down cycling in comparison to the Haber-Bosch process, which favors continuous operation because of the high temperature and pressure needed in the reactor.[8,18]

2.2. Transition metals as nitrogen dissociation catalysts

Whether following the Haber-Bosch process or the electrochemical route, ammonia synthesis uses a catalyst. Iron is most commonly used in the Haber-Bosch process, but there are other transition metals that can be used for this purpose.[12,13] The catalytic activity of these transition metals in nitrogen dissociation can be understood from molecular orbital theory. Molecular orbital theory explains chemical bonding of atoms into molecules.[21] Atoms have electron orbitals, which are quantum mechanical wavefunctions (solutions of the Schrödinger equation) around atomic nuclei. Two electrons fit into each orbital according to the Pauli exclusion principle. Molecular orbital theory entails the merging of electron orbitals belonging to covalent electrons into molecular orbitals spreading over all atoms in a molecule when atoms bond. These molecular orbitals are described as a linear combination of the atomic orbitals and can again accommodate two electrons, which form the covalent bond.[21]

For two atom molecules, like hydrogen and nitrogen, depending on the symmetry of the orbital, it is called a σ-orbital or a π-orbital; cylindrical around the line between two atomic nuclei (the internuclear axis) or perpendicular to this line respectively, which is similar to the symmetry of s and p atomic orbitals, hence the name. Each linear combination of two atomic orbitals from the two atoms, results in two molecular orbitals: one with constructive interference in the space between the two nuclei, which is a bonding orbital, and one with destructive interference, an antibonding orbital. This is visualized by the diagram on the left in figure 2.1. Electrons in bonding orbitals strengthen the covalent bond, while those in antibonding orbitals weaken it.[21] Like with atoms, electrons fill up the molecular orbitals starting with those of lower energy, where bonding orbitals have lower energy than antibonding orbitals. As long as there are more electrons in bonding orbitals than antibonding ones, the amount of which is called the bond order, the atoms can bond into a molecule. The bond order explains the lack of diatomic molecules of certain elements like helium and the height of the dissociation energy of diatomic molecules, in particular the high dissociation energy of the nitrogen molecule.[21]

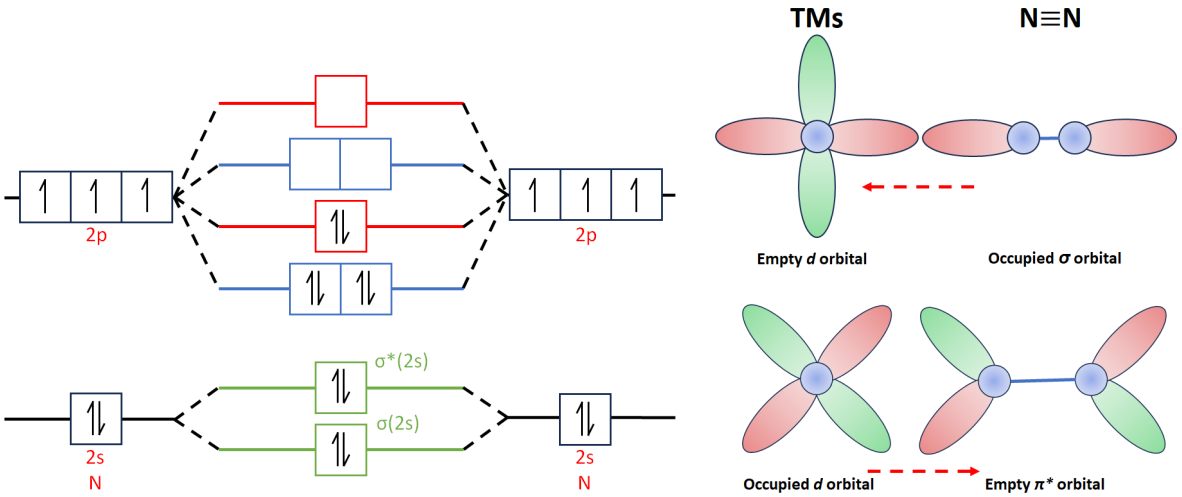

Figure 2.1: Molecular orbital theory explains the bonding of atoms into molecules and can be visualized using the diagram on the left. It shows a single nitrogen atom has 3 free valence electrons, which combine with the electrons of another nitrogen atom to fill the bonding orbitals of the nitrogen molecule, while the anti-bonding orbitals are empty. The diagram on the right shows the weakening of this bond by adsorption of the nitrogen molecule to a transition metal resulting in charge transfer to the anti-bonding orbitals of the nitrogen molecule. Courtesy to my daily supervisor P. Jungbacker for making this image.

The purpose of the catalyst in nitrogen reduction to ammonia is to lower the dissociation energy of the nitrogen molecule. Iron is one of several transition metals, along with nickel and ruthenium, that have strong catalytic activity due to the coexistence of empty and occupied d-orbitals.[22] This allows for the adsorption and activation of nitrogen by electron transfer from the occupied bonding orbitals of the dinitrogen molecule to the empty d-orbitals of the transition metal and from the occupied d-orbitals of the transition metal to the empty anti-bonding orbitals of the dinitrogen molecule, as shown in figure 2.1 on the right. This weakens or breaks the dinitrogen bond, allowing the nitrogen atoms to participate in reactions.[12]

It must be noted here, that these transition metals only have these partially occupied d-orbitals when they are sufficiently reduced. In other words, having a valence state of zero. In the presence of air or

water, transition metals like iron tend to oxidise, so keeping the metal on the surface of the catalyst reduced is essential. In the Haber-Bosch process, this is done by activating the catalyst beforehand using hydrogen gas , which reacts with oxides and hydroxides at elevated temperature and pressure, and by preventing access of water or oxygen to the catalyst surface.[19] In electrochemical ammonia synthesis however, metal reduction can be achieved electrochemically by using it as cathode in an electrochemical cell.[5]

To compare the different transition metals, they have historically been tested for catalytic activity. The activity depends on both the ease of adsorption and reduction of nitrogen and the ease of desorption of ammonia after the synthesis reaction is complete. These two requirements are at odds with each other, so there exists an optimum adsorption strength of nitrogen, often called the volcano plot relationship between adsorption strength and catalytic activity.[12,23] Iron should theoretically have the best performance for ammonia synthesis, since it is located near the optimum at the top of the volcano plot. Therefore, ammonia synthesis at the surface of an iron electrode will be the focus of this research.

2.3. Challenges in electrochemical ammonia synthesis

Besides the many benefits electrochemical ammonia production has over the Haber-Bosch process, it also comes with its own challenges. A number of these challenges are outlined in previous research at the MECS group by Ripepi *et al.*[5,13,15,16,24] As previously mentioned, one of the main challenges in electrochemical ammonia synthesis in an aqueous electrolyte is competition between the nitrogen reduction reaction and hydrogen evolution reaction. In alkaline electrolyte, these reactions are:

$4\,H_2O + 4\,e^- \longrightarrow 2\,H_2 + 4\,OH^-$ Hydrogen evolution reaction
$N_2 + 6\,H_2O + 6\,e^- \longrightarrow 2\,NH_3 + 6\,OH^-$ Nitrogen reduction reaction to ammonia

Using an aqueous electrolyte is desirable, because it can provide the hydrogen necessary for the reaction at the cathode through the dissociation of water ($H_2O \longrightarrow H^+ + OH^-$). In water electrolysis, in order to produce one oxygen molecule and two hydrogen molecules, a transfer of 4 electrons is needed. For electrochemical ammonia synthesis, not only must the triple bond of the nitrogen molecule be broken, 6 electrons are subsequently needed to produce two ammonia molecules. This means hydrogen more easily forms hydrogen gas, rather than being available for nitrogen hydrogenation.[5]

Other challenges occur when the nitrogen is blocked from reaching the catalytic surface. When using an electrode submerged in aqueous electrolyte, nitrogen needs to dissolve before it can reach the electrode surface. The concentration of dissolved nitrogen in water can be calculated from reported Henry's Law constants under standard test conditions of 298.15K,[25] which are defined as

$$H^{cp} = \frac{c_a}{p} \tag{2.1}$$

where c_a is the concentration of dissolved species and p is the partial pressure of that species in the gas phase under equilibrium conditions. In the experiments performed in this study, the partial pressure of nitrogen can be assumed to be close to 1 atm. In reality, the used nitrogen gas is not perfectly pure, but also the gas pressure is slightly higher than 1 atm to allow gas flow through the measurement setup. This results in an equilibrium nitrogen concentration of $6.4 \cdot 10^{-4}$ mol/L. Based on the molar weight of water of 18g/mol and the same standard test conditions of 298.15K and 1 atm of pressure, where 1g of water is roughly equal to 1ml of water, the water concentration is about 55.6mol/L. This results in almost 87000 times more water than nitrogen present at the electrode surface. When the concentration of nitrogen is this low, the attempt frequency of nitrogen reaching the surface is also low, leading to a low reaction rate. When a nitrogen molecule does reach the adsorption sites on the electrode surface, they are limited according to the Langmuir adsorption theory. Following this theory, the probability of nitrogen sticking to the surface goes down depending on the surface coverage, which is the fraction of blocked adsorption sites. The sticking probability is denoted by

$$S = (1 - \theta)s_0 \tag{2.2}$$

where θ is the fractional surface coverage and s_0 the sticking probability on a perfectly clean surface. The surface coverage θ is partially dependent on the temperature and the partial pressure of the adsorbate. In the case of nitrogen adsorption on the surface of an iron electrode in an aqueous electrolyte, the adsorption sites can also be blocked by other species besides the adsorbate, such as

synthesized ammonia before desorption or NH_x in intermediate steps from nitrogen to ammonia. This results in a lower sticking probability and therefore a lower reaction rate.

2.4. Previous research at the MECS group

The nickel hydrogen permeation electrode setup previously used in the MECS group to tackle these challenges is shown in Figure 2.2. The electrode separates the water dissociation reaction and nitrogen reduction reaction on both sides of the electrode and atomic hydrogen permeates through the electrode to the nitrogen gas side, where it reacts with adsorbed nitrogen or surface nitrides to produce gaseous ammonia.[5,13] The used nitrogen or surface nitrides leave behind a vacancy for new nitrogen atoms to adsorb to continue ammonia synthesis, which is called a Mars-van Krevelen mechanism. This mechanism is the reason nickel was used as electrode material instead of iron. While the use of an iron electrode in this setup was attempted, the surface nitrides, as well as difficulty in reducing the iron surface, were shown to block atomic hydrogen permeation. The benefit of such a setup is the lack of poisoning of the catalytic sites on the electrode surface for nitrogen absorption and activation. There is no adsorption of water or oxygen on the gas side while atomic hydrogen is still available despite the separation between the aqueous electrolyte and the nitrogen reaction sites. Also, nitrogen does not need to dissolve to access the electrode surface and any ammonia produced cannot dissolve into the electrolyte as well.

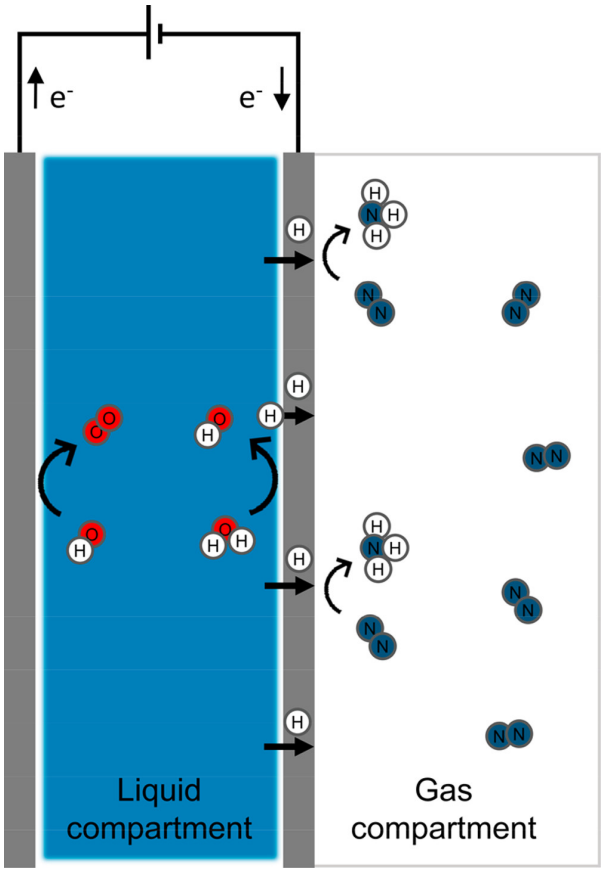

Figure 2.2: The setup used previously in the MECS group for ammonia synthesis, with a separate gas and liquid chamber. The thin nickel electrode separates the water dissociation reaction and nitrogen dissociation reaction on both sides of the electrode. Atomic hydrogen permeates through the electrode to react with adsorbed nitrogen at the gas-electrode interface.[5]

2.5. Using a porous iron electrode for electrochemical ammonia synthesis

Although the method described above shows promise for ammonia synthesis, the ammonia yield can still be improved. Hydrogen permeation also necessitated the use of Ni, which is not a traditional ammonia synthesis catalyst, to obtain a reduced transition metal surface. In particular, increasing the catalytic surface area of a reduced Fe^0 surface can allow for more active sites for nitrogen adsorption and reduction. Therefore a porous iron electrode could be promising for ammonia synthesis. Since the electrode will be porous, both gas and aqueous electrolyte will be able to flow through it. Access of the electrolyte to the intended catalytic iron surface can allow for the successful reduction to Fe^0, however the electrode will no longer be able to completely separate the two compartments like in figure 2.2. Therefore, the porous iron electrode should be used in a horizontal setup, by positioning the electrode on top of the electrolyte surface. Instead of atomic hydrogen permeation, gravity and the capillary force of the electrolyte sucking into the pores will make a region where both aqueous electrolyte and gas can access the surface, without nitrogen dissolution and diffusion through the electrolyte being a limiting factor since the gas and electrolyte are still separate. Using a KOH solution as electrolyte includes the added benefit of having K^+ near the surface, which in the Haber Bosch catalysis case has a positive effect on the ammonia synthesis.[26] In order to limit competition from the hydrogen evolution reaction in this setup, the optimal potential to be applied to the electrode should be determined. Besides supplying the necessary energy to reduce water to adsorbed H and OH^-, form NH_x and ammonia, the applied potential also keeps the iron surface reduced. The N_2 activation to adsorbed N, however, is not potential driven, but should result from the bonding-anti-bonding orbital effects between N_2 and the Fe^0 surface.

The limiting potential for the Fe^{2+} to Fe^0 reduction that needs to be applied to the iron electrode can be understood from a Pourbaix diagram. This is a diagram showing the stability of different valence states of an element in an aqueous electrolyte as a function of pH and potential applied versus a standard hydrogen electrode (SHE) as a reference. Figure 2.3 shows the Pourbaix diagram of iron in an aqueous electrolyte. The dashed lines are hydrogen and oxygen stability lines. At electrode potentials below the bottom dashed line, the hydrogen evolution reaction (HER) can occur. A reversible hydrogen electrode (RHE) also used this line as a reference. From figure 2.3 can be concluded that in an alkaline environment, the stable region of reduced, metallic iron is close to the hydrogen stability line. This means only a small potential difference, in the order of -0.1 V versus a hydrogen reference electrode, is needed to keep iron reduced.

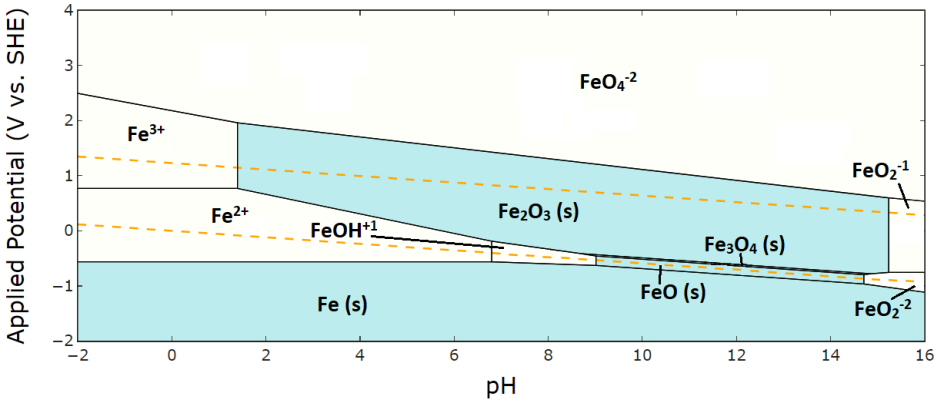

Figure 2.3: Pourbaix diagram of iron in an aqueous electrolyte. The top and bottom dashed lines are the oxygen and hydrogen stability lines respectively. The blue shaded areas indicate a solid, whereas the white areas are dissolved species. Around pH 14, iron can be reduced by applying a potential slightly below the hydrogen stability line. Figure was made with the help of the Pourbaix diagram tool of the Materials Project.[27]

To determine if ammonia can be formed at this electrode potential, the Pourbaix diagram of nitrogen must be consulted. Figure 2.4 shows the Pourbaix diagram of nitrogen in an aqueous electrolyte. Two points can be concluded from this diagram. First, it shows ammonia will dissolve and form ammonium ions in neutral or acidic conditions. This is one of the reasons an alkaline electrolyte is necessary.

Another reason is it discourages ammonia from dissolving into the electrolyte following Henry's Law.[28] Second, when comparing the Pourbaix diagram of nitrogen with the one of iron, it can be concluded that nitrogen can react to ammonia at the potentials required to keep iron reduced, which is slightly below the hydrogen stability line at about -0.1V versus a reversible hydrogen electrode (RHE). In fact, the equilibrium potential for NH_3 formation is less negative than for H_2 evolution. So at the potential where Fe^0 is stable, the overpotential for NH_3 formation is slightly higher than for H_2 formation, meaning ammonia synthesis could be favored over the HER. By not applying a potential lower than this, competition from the HER can be limited. Not only the exchange current for H reduction is relevant for a reaction rate, but also the availability of adsorbed N, and this study aims to determine if the latter is the limiting factor in electrochemical ammonia synthesis.

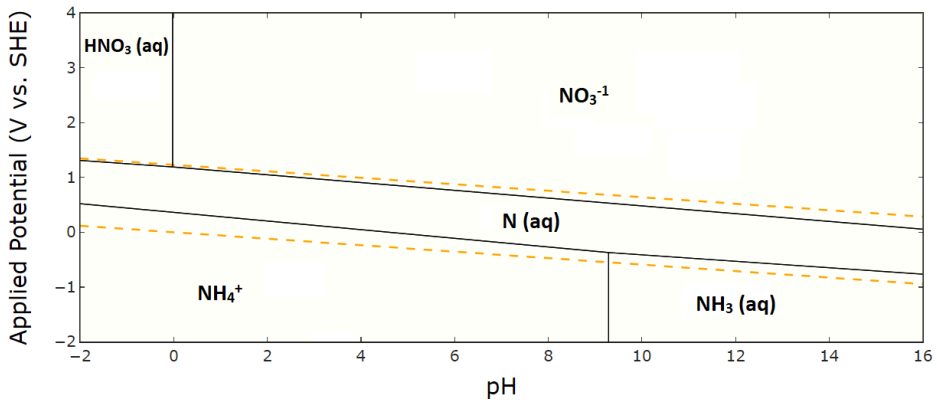

Figure 2.4: Pourbaix diagram of nitrogen in an aqueous electrolyte. The top and bottom dashed lines are the oxygen and hydrogen stability lines respectively. At pH 14, potentials slightly below the hydrogen stability line result in ammonia formation from atomic nitrogen. As long as an iron catalyst breaks the triple bond of the nitrogen molecule, atomic nitrogen will be available to form ammonia. Figure was made with the help of the Pourbaix diagram tool of the Materials Project.[27]

2.6. Experimental methods and contamination concerns

Now that the combination of the right potentials, a reduced iron surface, nitrogen access to the electrode and alkaline electrolyte are determined, ammonia production in the gas phase is expected to be possible. In order to test the performance of such an electrochemical cell, samples of both the gas phase and liquid phase must be taken and tested for the presence of ammonia during operation of the electrochemical cell. When performing these measurements, one of the challenges commonly encountered in research is contamination by nitrogen containing compounds. These compounds cause false-positive results where the production of ammonia is due to the contamination instead of the nitrogen reduction of nitrogen gas supplied during the experiment. Common sources of contamination are nitrogen oxides NO_x present in the gas supply,[29] dissolved in the electrolyte, present in/adsorbed on the electrode material,[30] or present on glassware used for the experiment.[31] These nitrogen contaminations already contain activated nitrogen, meaning there is no triple bond making the molecule inert. In order to ensure ammonia synthesis happens due to the nitrogen reduction reaction at the working electrode, it is necessary to detect and remove possible contaminants. In this research, ion chromatography (IC) measurements are used to detect nitrate and nitrite in the electrolyte before the start of the experiment. Since ammonia produced in this setup can potentially also dissolve into the electrolyte and be oxidised at the counter electrode, these IC measurements of the electrolyte are also repeated after the experiment.

In addition to measuring nitrate and nitrite, dissolved ammonia can also be measured directly using nuclear magnetic resonance (NMR) spectroscopy. The method used has previously been developed in the MECS group by Kolen *et al.*[32] There are different types of NMR spectroscopy, but in general an NMR measurement works by putting a thin glass tube containing a small amount of liquid sample in a strong magnetic field. This aligns the magnetic spin of the atomic nuclei with non-zero nuclear spin. These nuclei have different angular momentum energy levels. This alignment is then perturbed by a much weaker oscillating magnetic field in the form of an electromagnetic pulse, when the energy of the

pulse equals the difference between two energy levels of the nucleus. This perturbation causes the atomic nuclei to resonate and emit electromagnetic waves, which can be detected. For the detection of dissolved ammonia, an Agilent 400MHz spectrometer is used. 400 MHz is the resonance frequency of a proton in the magnetic field of the spectrometer, which is a measure of the field strength the spectrometer produces. A proton is the nucleus of a ^{1}H atom. Measuring the response of these atoms is one of the most common types of NMR spectroscopy and was also the type used for detection of ammonia. The chemical environment of the atom results in small changes to the resonance frequency of the atom, making NMR spectroscopy a useful tool in detecting different chemical species. These small changes are in the order of Hz and are proportional to the magnetic field of the machine. To produce a machine independent spectrum, these small changes in resonance frequency are divided by the frequency of the spectrometer, 400 MHz, to obtain a small number. This number is multiplied by one million and given the units parts-per-million (ppm). The typical result of an NMR spectroscopy measurement is therefore a spectrum with ppm on the x-axis and intensity on the y-axis, denoting the intensity of the response from ^{1}H atoms at each frequency. In order to prevent the spectroscope from measuring the hydrogen atoms of the solvent, which is not of interest, deuterated solvents are used, where the hydrogen atoms are replaced by deuterium, which have a different nucleus. Following the method of Kolen *et al.*, deuterated dimethylsulfoxide (DMSO-d6) was used. This is one of the more common solvents used, making it easier to identify peaks in the spectrum from trace impurities, since most are known.[33] The method used is quite successful as well in suppressing the response from water present in the dissolved sample.

As shown by Kolen *et al.*, the final NMR sample to be analysed has to be acidic, because dissolved ammonia turns into ammonium ions at lower pH, as the Pourbaix diagram in figure 2.4 also clearly shows. The presence of ammonium ions NH_4^+ gives three distinct peaks in the spectrum, as shown in figure 4.3.[32] Maleic acid of known concentration is also added to the sample to determine the ammonia concentration. The integral of the three measured intensity peaks belonging to ammonia are translated to a concentration by comparing to the integral of the peak belonging to maleic acid. The concentration can the be calculated from equation 2.3.

$$C_{\mathrm{NH_4}^+} = \frac{I_{\mathrm{NH_4}^+}}{I_{MA}} \frac{N_{MA}}{N_{\mathrm{NH_4}^+}} C_{MA} = \frac{I_{\mathrm{NH_4}^+}}{I_{MA}} C_{MA} \tag{2.3}$$

In this equation, C is the concentration of each chemical species, I the integral of the corresponding peak and N the number of protons in each species, which is the same in NH_4^+ and maleic acid, canceling out the term.

If no contamination of the electrolyte due to nitrogen containing compounds and ammonia dissolution into the electrolyte can be detected, any produced ammonia will be present in the gas stream. Gas samples will be tested for the presence of ammonia using gas chromatography coupled with mass spectrometry following a procedure used by Ripepi *et al.*[15,16].

3

Experimental setup

The experiments performed can be divided into several steps. First is the production of the iron electrode used for subsequent experiments. The porosity of the electrode was measured to determine if it indeed has the increased catalytic surface area needed. Next is a description of the setup used for initial cycling experiments with the electrode to test if the iron can be reduced electrochemically. Finally, this chapter includes a description of the flow cell setup used for ammonia synthesis and its connection to the gas chromatography-mass spectrometry (GC-MS) machine.

3.1. Production of the sintered iron electrode

The iron electrode used for the electrochemical ammonia synthesis is made from a paste consisting of 55 wt% iron (Carbonyl iron powder). The rest consists of carbon black, agar, sodium tetraborate and water. Presenting an overview of the ratio of ingredients, table 3.1 contains the amounts used in a typical production run for the sintered iron electrode. At least 4 electrodes can be made using these amounts.

Table 3.1: Amounts of chemicals used for creating electrode paste, when dissolved in about 28ml of water. Excess water can be easily evaporated, but the ratio of chemicals added must be followed as shown here.

Chemical	**Amount (grams)**
Carbonyl Iron	26.3
Carbon Black	0.86
Agar	0.60
Sodium tetraborate decahydrate	0.11

Agar is a polysaccharide that is used as binder in this electrode. The carbon black is used for electrical conduction and 3.14 % of the total iron and carbon weight is added. The agar and sodium tetraborate are dissolved in water kept at 95 degrees Celsius using a water bath and added together while stirring until a mixture of 3 wt% agar and 0.3 wt% sodium tetraborate is made. First iron and then carbon are stirred into this mixture. The elevated temperature is necessary to keep the paste fluid. The mixture needs to be covered to prevent excessive evaporation.

The paste can be injected into a mould using a syringe to create a desired porous shape or spread into a flat slab. Both of these shapes were used in this study. After drying with acetone, the electrodes are put in a tube oven under an atmosphere of argon with 5 % hydrogen gas. Before the actual sintering, the temperature is increased to 300 °C at 5 °C/min and holding this temperature for an hour for debinding. This burns away most of the agar and water. Then the electrodes are sintered by increasing the temperature 1 °C/min until 800 °C, after which the temperature is held constant for 2 hours, before cooling down naturally. Storing leftover paste was also attempted, but electrodes made from stored paste did not perform as well in consequent cycling experiments in an electrochemical cell, reaching a lower energy capacity. Therefore, using fresh paste for sintering is recommended. The resulting

electrodes are shown in figure 3.1. Pictures were taken after extended use in experimental setups, without showing visible changes to the electrodes, which indicates their stability.

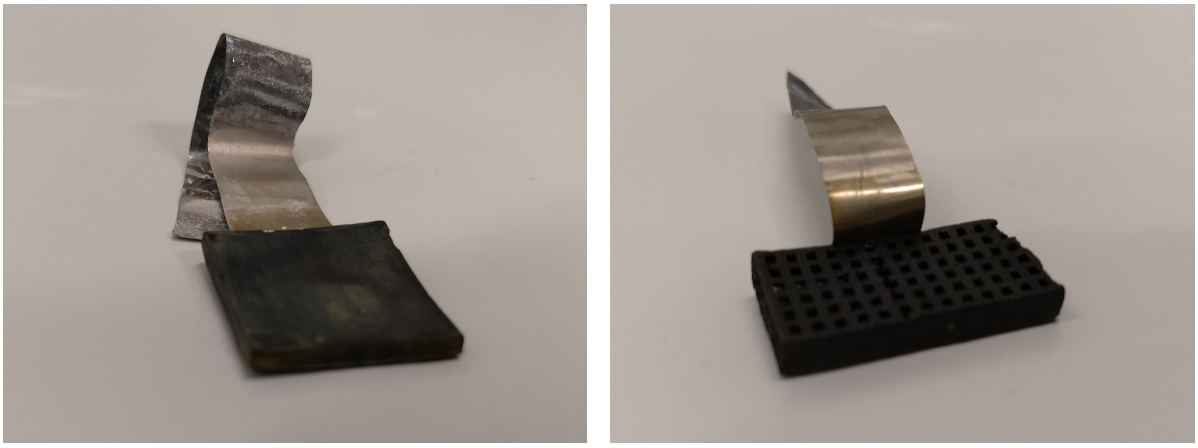

Figure 3.1: Images show the two shapes of porous iron electrodes used in this study. Pictures were taken after extended use in experimental setups. The electrodes were made from a paste using a mixture of chemicals shown in table 3.1 and sintered in a tube oven at temperatures of up to 800 °C. Ni current collectors were attached using spot welding.

Since an increased catalytic surface area is one of the primary reasons for performing this research, simple tests were performed to determine the porosity of the produced iron electrodes. The volume of a simple slab electrode can be easily calculated. It has typical measurements of 22mm by 22mm by 2.5mm. By measuring the weight of the electrode, the density can be determined and compared to the density of pure iron. This results in porosities of between 67% and 75%. Alternatively, the electrode can be submerged in isopropanol for 10 minutes. Comparing the weight before and after submerging, results in the weight of isopropanol absorbed by the electrode. By calculating the volume of isopropanol absorbed and comparing to the total volume of the electrode, the porosity can be determined. This results in porosities between 57% to 85%, which is the percentage of volume that is not filled with isopropanol. These results indicate the electrode material resulting from the sintered paste is at least somewhat porous, which should increase the available electrode surface.

3.2. A simple electrochemical cell setup for cycling experiments

Since the presence of reduced iron is essential for the success of electrochemical ammonia synthesis, the slab-shaped electrodes were first tested in a simple electrochemical cell setup to see if the iron can be reduced electrochemically. This setup consists of a plastic container filled with 1M potassium hydroxide as aqueous electrolyte. The sintered iron working electrode and stainless steel or nickel foam counter electrode were submerged into the electrolyte and connected to the outside of the container through nickel current collectors. The current collectors were connected to a MACCOR battery cycler device.

In order to place the electrode on the electrolyte surface to allow for gas contact, a plastic structure submerged in the electrolyte was introduced to the simple electrolyte setup. A schematic representation of this setup is shown in figure 3.2. The counter electrode was placed below the plastic structure on the bottom of the container. The air inside the container above the electrode surface can be replaced with pure nitrogen gas.

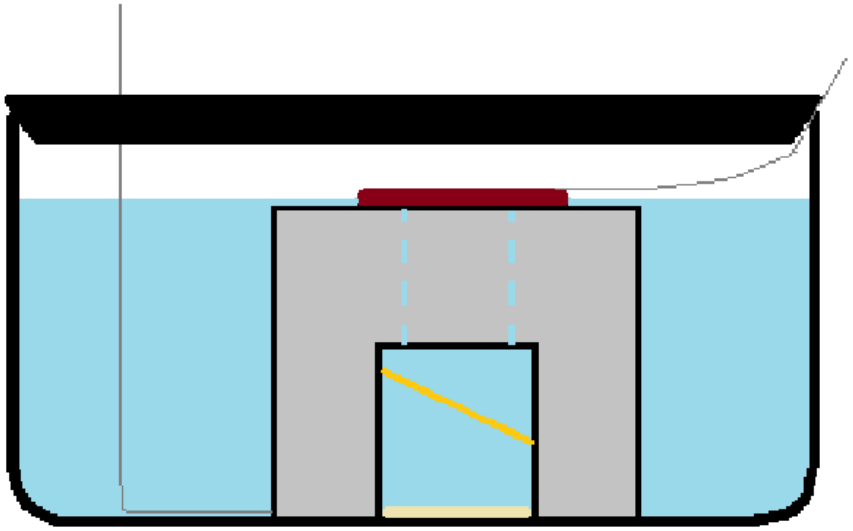

Figure 3.2: Schematic of the simple electrochemical cell with plastic structure (grey). The slab electrode lies horizontally on the plastic structure at the same height as the electrolyte surface, allowing electrolyte and gas contact with the electrode. The electrode lies on top of a hole in the plastic surface, allowing contact to the bulk electrolyte. The counter electrode lies on the bottom of the container beneath the plastic structure. A Zirfon membrane is lodged into the plastic structure in between the two electrodes to prevent O_2 gas bubbles formed at the counter electrode to reach the working electrode and block its electrolyte access.

3.3. A cell setup with a dedicated gas outlet

The cell setup with plastic structure does have a few limitations. It results in gas bubbles being trapped underneath the iron working electrode, partially blocking its connection to the electrolyte. The cell is also difficult to make airtight, resulting in possible contamination from airborne nitrogen oxides NO_x. Most importantly, while it is possible to take electrolyte samples from the cell to measure dissolved ammonia, it lacks a dedicated gas outlet to test for synthesis of ammonia gas. For these reasons, a dedicated flow cell design was used, as depicted in figure 3.3.

This cell consists of a working electrode and counter electrode compartment, separated by a Zirfon membrane held in place by gaskets. The membrane is used to prevent gas exchange between the compartments, since oxygen gas formed at the anode could poison the reaction sites on the cathode surface and ammonia gas formed at the cathode can leak away to the anode compartment. Both compartments have a separate in- and outlet for pumping liquid electrolyte. The working electrode compartment also has a gas inlet. This allows both electrolyte and gas to flow through the system and access the electrode surface. The nickel foam counter electrode is connected to the outside of the compartment by nickel foil sandwiched by gaskets. The porous iron working electrode is similarly connected by nickel foil. The shape of the electrode was changed to a porous structure using a mould. This allows gas bubbles to move through the electrode and also increases the surface area even further. Alternatively, the entire setup can also be put on its side with the cathode compartment on top, resulting in the formation of a separate gas layer in the cathode compartment. This allows the electrode to be positioned on top of the electrolyte surface, as seen in part d of figure 3.3, which allows for greater and prolonged gas access to the electrode surface.

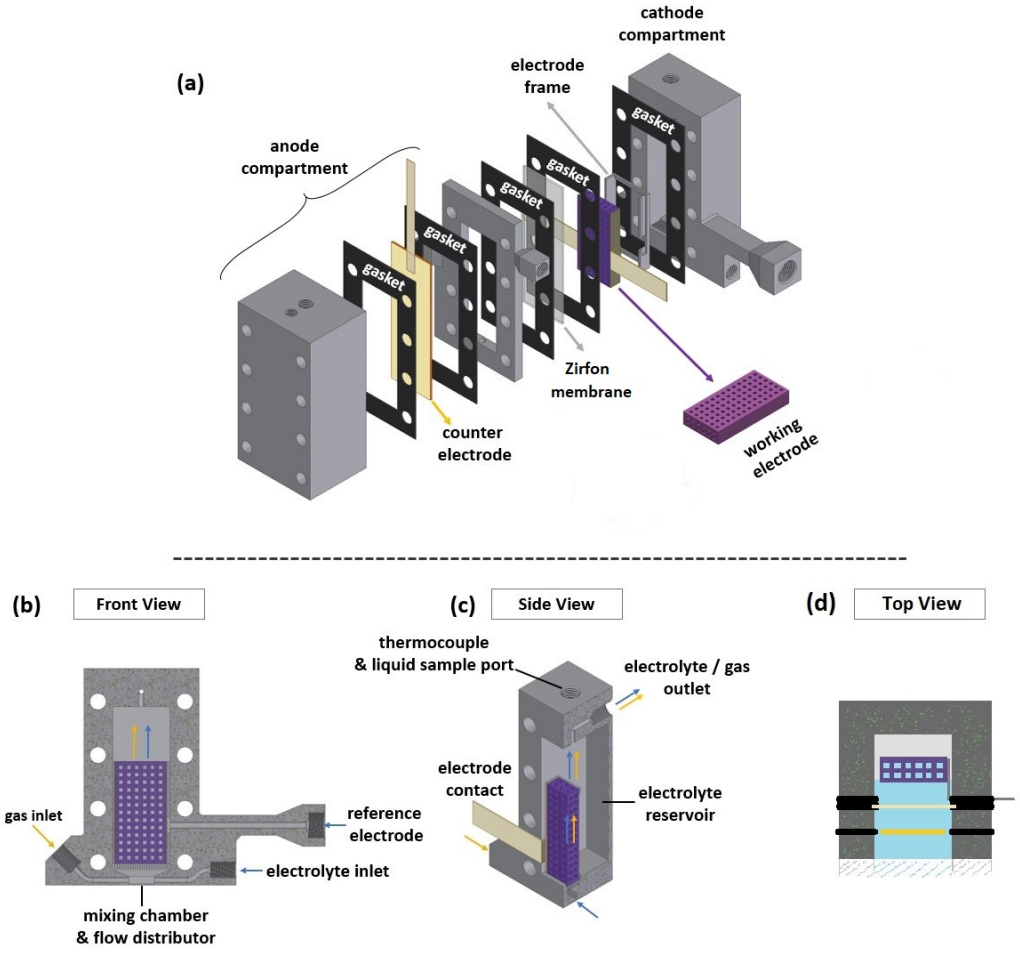

Figure 3.3: Schematic of the flow cell used for ammonia synthesis experiments allowing for a controlled gas flow to be able to measure ammonia in the gas phase. The cell consists of an anode and a cathode compartment separated by a Zirfon membrane to prevent gas exchange between the compartments. Figure a shows an overview of the entire cell. Figure b is a front view inside the cathode compartment, including a separate mixing chamber for gas and electrolyte. Figure c shows the cathode compartment from the side, including the electrolyte/gas outlet. Figure d shows a top view of the cell. When the cell is turned on its side with the cathode compartment on top, it is filled with a separate gas and electrolyte layer.

The electrolyte in- and outflow of the two compartments are connected to two separate plastic containers with electrolyte using Teflon tubing. Electrolyte flow is achieved using a peristaltic pump. Gas flow speed at the inlet is controlled by a gas flow controller. Input gas flows through the working electrode compartment and ends up in the electrolyte container. From this container, the gas leaves the system through a tube connected to a gas chromatography-mass spectrometry (GC-MS) machine. A schematic of the setup is shown in figure 3.4. To prevent ammonia from physisorption to the tube walls anywhere in the setup and contaminating future experiments, either Teflon tubing or coated stainless steel tubing is used. A PTFE membrane is used as a water filter to block liquids from entering the GS-MS machine.

An oxygen and moisture trap was added to the flow cell setup, to ensure the gas input is free of contamination. The use of an oxygen/moisture trap has been successful in the MECS group in the past to remove nitrogen containing compounds in the nitrogen gas supply as well.[24] The two electrolyte containers were made airtight, ensuring no airborne nitrogen contamination can enter the setup during the experiment. As explained in chapter 2, samples of the electrolyte were tested for the presence of nitrite and nitrate, both before and after some experiments, using ion chromatography. Nuclear magnetic resonance spectroscopy experiments were performed on the same samples using a specially prepared solvent according to the specifications of Kolen *et al.*, to ensure the sample is sufficiently acidic and contains a known concentration of maleic acid.[32]

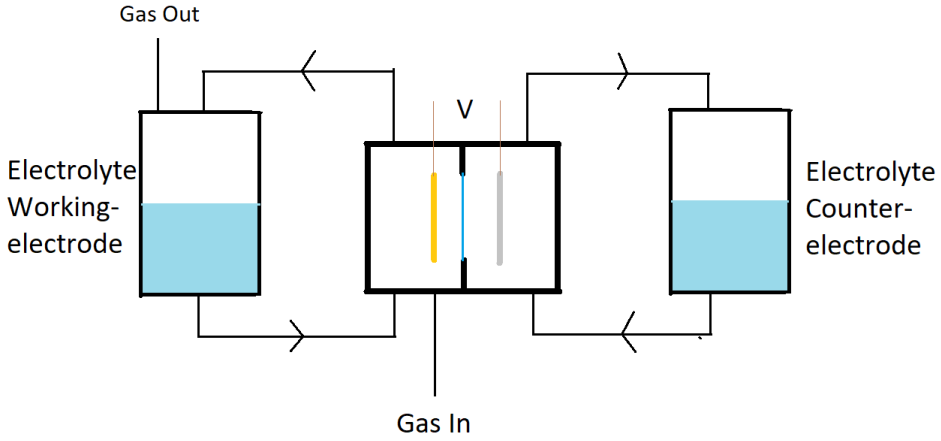

Figure 3.4: Schematic overview of the flow cell measurement setup, showing the flow cell in the middle, with a porous iron working electrode and nickel foam counter electrode in chambers separated by a Zirfon membrane. The flow cell has a separate gas inlet and both chambers have an electrolyte in- and outlet. Gas flows past the working electrode, through the electrolyte outlet to the working electrode electrolyte container, which has a separate gas outlet.

4

Results

As explained in section 2.5, before ammonia synthesis can be attempted, the surface of the iron electrode must be shown to be sufficiently reduced. Therefore, this chapter will start with the results from electrode cycling experiments. Then the measurements of nitrogen containing compounds in the electrolyte will be discussed. Finally, there are the results of ammonia detection in the gas flow.

4.1. Cycling of the electrode

The simple, plastic container electrochemical cell setup was used to test the electrochemical activity of the sintered iron electrode. The cell was cycled through numerous charge and discharge steps: 8h of charging with a constant current of 50mA followed by discharging at 50mA until a cell voltage of -0.6V was reached. Discharging had to be limited in this way to prevent the Fe^{2+}, formed on the electrode surface during discharge, from reacting further into Fe^{3+}. This reaction can become irreversible, so the iron on the electrode surface must be cycled between its 0 and 2+ valence states to prevent the loss of electrochemical activity of the iron surface. This procedure is used to obtain a large and porous reduced Fe surface on these electrodes.

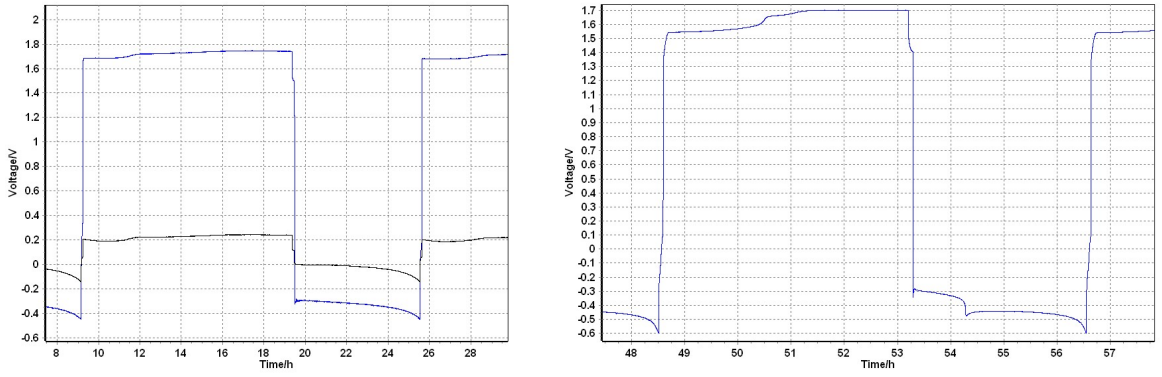

(a) (b)

Figure 4.1: Results of electrode cycling experiments using a fixed current of 50mA. The porous iron electrode and nickel foam counter electrode were submerged in a 1M KOH electrolyte. Note that the cathode is reduced during the charge step, which is defined as having a positive voltage. After an initial charge phase of 8h, the cell was repeatedly charged and discharged, where discharge steps continued until a lower voltage limit was reached and charge steps continued until twice the current capacity of the previous discharge step to ensure maximum reduction of the iron surface. The left graph shows the cell voltage in blue and working electrode potential versus RHE in black during one cycle of reduction and oxidation of the iron in the charge and discharge steps. The right graph shows the cell voltage during one cycle where the electrode is discharged until Fe_3^+ forms.

Figure 4.1a shows a graph of the cell voltage of a typical cycling experiment using the sintered iron electrode. Note the voltage becomes positive when charging and negative when discharging, which is opposite to the Pourbaix diagram in figure 2.3 because of how the cables are connected to the

MACCOR battery cycler. During charging, iron is reduced to its zero valence state. The voltage slowly increases until full capacity is reached at around 1.7V, where the voltage graph becomes horizontal and only water splitting occurs. After a rest step of a few minutes, the following discharge step starts as a nearly horizontal curve, but the slope increases downward over time. In this phase, iron is oxidised into its 2+ valence state. Continued discharging results in iron entering the 3+ valence state, indicated by a second plateau in figure 4.1b.

Discharge capacities of 300 mAh/g were reached, indicating significant electrochemical activity on the electrode surface: Fe^{2+} created during discharging can be successfully reverted in the charge step to Fe^{0}, which is needed as catalyst for ammonia synthesis. This result shows it is indeed possible to create a reduced iron surface electrochemically. Another result of these measurements is the excellent contact of the electrode with the electrolyte even when partially above the electrode surface, like in the side-ways configuration of the flow cell. Figure 4.2 shows two graphs at the top, which are a comparison of two cycles of the same slab-shaped electrode at a fixed current of 50mA in both the charge and discharge step. The left graph is a cycle with the electrode fully submerged, while the right graph is a cycle with the electrode placed on top of the plastic structure, where only one side of the electrode is in contact with the electrolyte. The stable voltage at which water splitting occurs during the charge step increases with 0.15V when the slab electrode is partially outside the electrolyte. Similarly, the discharge step also occurs at a 0.15V lower voltage. This indicates only a small increase in resistance as a result of decreased electrolyte contact. For the porous-shaped electrode in the flow cell setup, the bottom graph of figure 4.2 shows the cell voltage zoomed in on the moment the cell is turned during the measurement. There is a small voltage peak, but the cell voltage returns to the same level afterwards, despite having only one side in contact with the electrolyte. This indicates the electrolyte is wetting the entire electrode, which is porous enough for ion diffusion from one side to the other.

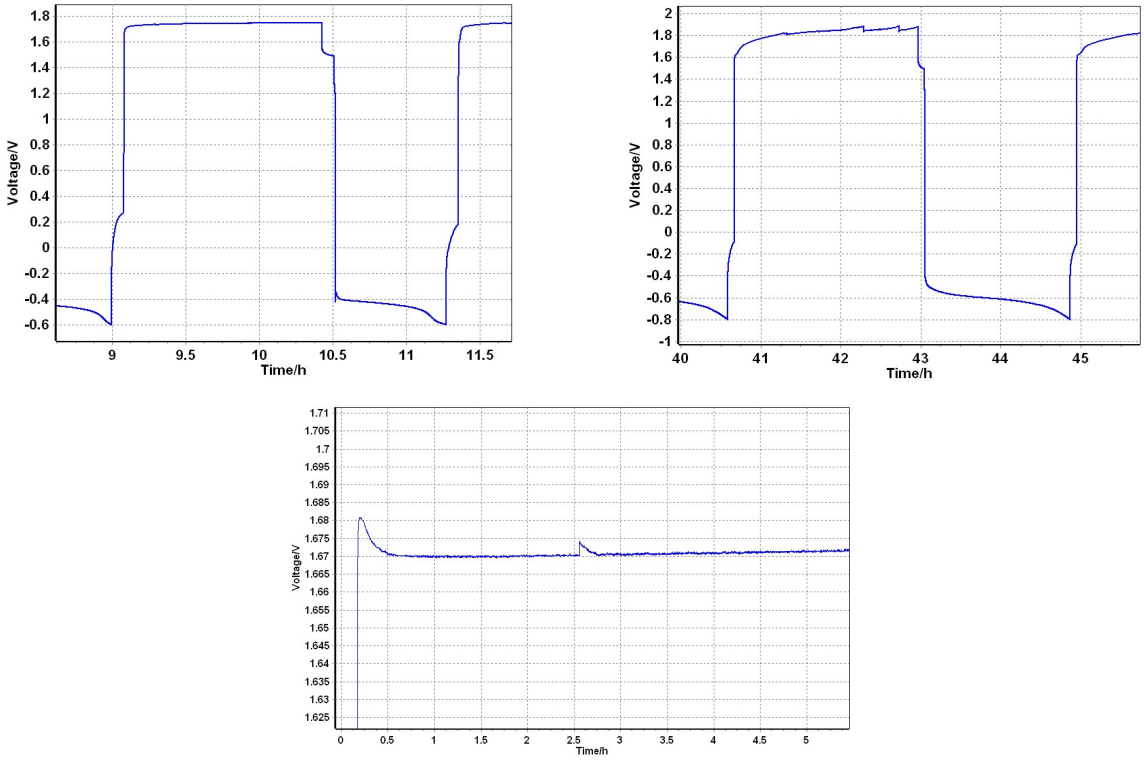

Figure 4.2: Results of electrode cycling experiments using a fixed current of 50mA and 1M KOH as electrolyte. Note that the cathode is reduced during the charge step, which is defined as having a positive voltage. The top two graphs show the differences in cell voltage during cycles of the same slab-shaped electrode, with the electrode fully submerged for the left graph and only one side in contact with the electrolyte for the right graph. The bottom graph shows the cell voltage of the flow cell setup during a charging step. When the cell is turned on its side just after 2.5 hours, only a small peak in the voltage appears, after which the voltage returns to its previous value. This indicates the excellent contact between the entire electrode and the electrolyte even when only one side touches the electrolyte surface.

4.2. NMR measurements of the electrolyte

Figure 4.3 shows an example of part of a NMR spectrum if ammonia is present in the sample. This spectrum was measured to try and reproduce the method of Kolen *et al.*[32]. A few NMR spectroscopy measurements failed, when the pH was too high, so the acidification of the sample is necessary.

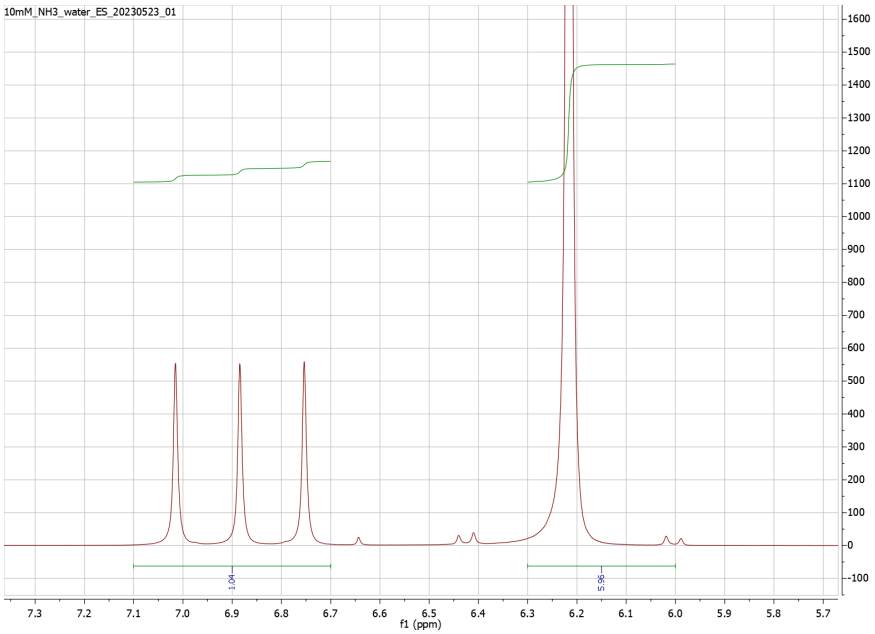

Figure 4.3: NMR spectrum of 10 mM of ammonium nitrate dissolved in water. This indicates the locations of the peaks in the spectrum if ammonia were to be dissolved in the electrolyte. The relative peak areas of the ammonia and maleic acid peaks are also indicated to be 1.04 and 5.96 respectively.

Electrolyte samples from experiments using both electrochemical cell setups were taken, including samples from fresh electrolyte before the start of an experiment. The ammonia peaks from these measurements are only barely recognizable from background noise and there is no measurable change in ammonia concentration before and after ammonia synthesis experiments. This makes the calculation of the integral unreliable, but it does show the amount of ammonia present in the electrolyte to be negligible. This means there was either little or no ammonia produced, the ammonia produced did not dissolve, but was in the gas phase, or the dissolved ammonia easily reaches the counter electrode where it oxidizes into nitrate or nitrite.

4.3. Ion chromatography measurements for nitrate and nitrite contamination in the electrolyte

Based on previous measurements by Ripepi *et al.*, a 10 ml sample of fresh 1M KOH electrolyte inside a typical setup for nitrogen reduction has 140 nmol of nitrogen containing compounds, mostly NO_x impurities.[24] This is a concentration of 14µM. Comparing to this research, ion chromatography (IC) measurements of fresh electrolyte have shown 0.4µM of nitrite. IC measurements of the electrolyte from the flow cell after being in contact with an N_2 gas layer in the cathode compartment for 2 days resulted in an NO_x content of 5.1µM (±0.5µM). This measurement was taken after one ammonia synthesis experiment, where small amounts of ammonia were detected in the gas. Another six days later, the NO_x content in the electrolyte has risen to 7.8µM (±2.0µM). It can be concluded from these measurements that the nitrogen contamination in the electrolyte is negligible and no significant amounts of ammonia were produced in the dissolved state, as seen from both NMR and IC measurements.

4.4. Gas chromatography measurements

Because both the amount of dissolved ammonia found with NMR spectroscopy and the amounts of nitrate and nitrite found using ion chromatography are negligible, any ammonia produced should be found in the gas phase. These ammonia synthesis experiments are performed at a fixed current of 1mA, corresponding to a 0.07V potential applied to the working electrode versus the hydrogen reference electrode and a cell voltage of 1.47V. Gas chromatography measurements using the flow cell setup typically yield a spectrum like the one shown in figure 4.4. The large, wide peak in the middle of the spectrum is caused by water vapor in the gas sample. Even though a PTFE membrane was used as water filter in between the flow cell and gas chromatograph, there is still a large peak because this filter blocks liquid water droplets while it transports water vapor that is able to pass the filter. The size and width of this peak can vary, but the ammonia peak of interest is always found around 0.04 minutes before this water peak, usually around 1.65 minutes.

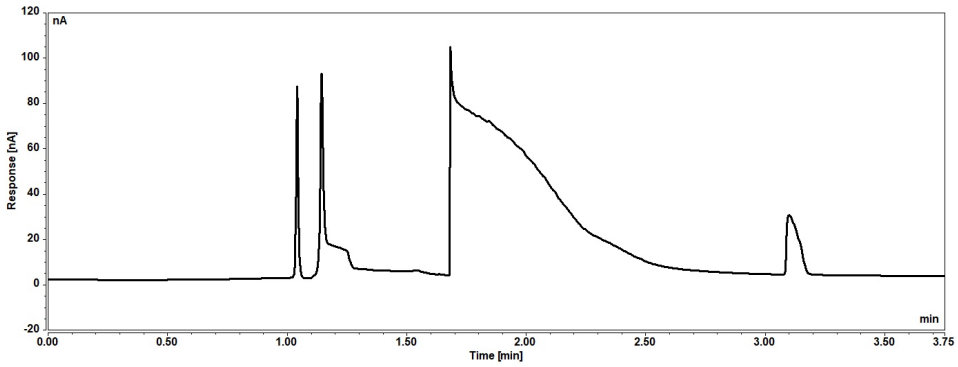

Figure 4.4: Full gas chromatography spectrum of a typical ammonia synthesis experiment. The large peak in the middle is due to water vapor. Ammonia should appear just before this peak. Ammonia synthesis experiments were performed at a fixed current of 1mA corresponding to a 0.07V potential difference of the working electrode versus the hydrogen reference electrode and a cell voltage of 1.47V. Electrolyte flow through the cell was 0.5 ml/min in both the cathode and anode compartment and gas flow varied between 0.13 and 0.5 ml/min.

When using the flow cell in the upright position and nitrogen gas bubbles through the 3D porous iron electrode, no ammonia was detected in the gas chromatography measurements. Only in the sideways configuration, when a small volume of about 13cm^3 of nitrogen gas is trapped inside the cell and in contact with the electrode surface for several hours, does a measurable amount of ammonia accumulate in the gas. Inserting this gas into the gas chromatograph with a gentle gas flow of 0.2-0.5 ml/min through the flow cell results in a small peak as shown in figure 4.5. This peak is visible for 5-10 back-to-back injections into the gas chromatograph.

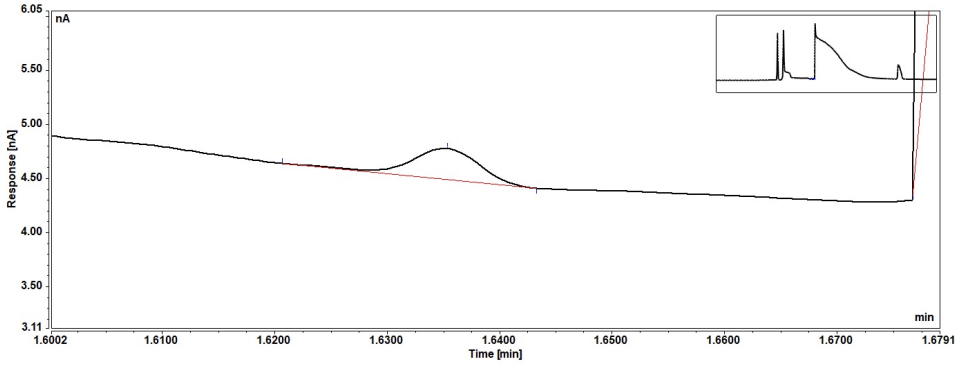

Figure 4.5: Part of a gas chromatography spectrum zoomed in on a peak belonging to ammonia detection. Ammonia synthesis experiments were performed at a fixed current of 1mA corresponding to a 0.07V potential difference of the working electrode versus the hydrogen reference electrode and a cell voltage of 1.47V. Electrolyte flow through the cell was 0.5 ml/min in both the cathode and anode compartment and gas flow varied between 0.13 and 0.5 ml/min.

Despite efforts to detect and eliminate sources of nitrogen contamination in advance, an additional test was performed to detect if some contamination is still present. Filling the flow cell with Ar instead

of N_2 gas, should remove the only source of nitrogen in the system, since only negligible ammonia and nitrides were measured in the electrolyte, even after operating the cell with N_2 gas for hours. The flow cell was flushed with an Ar gas flow of 10 ml/min for several hours to remove all traces of the nitrogen gas still present. The previous experiment was then repeated with the flow cell having a small volume of Ar gas trapped inside. Curiously, the subsequent gas chromatography measurements indicated a similar buildup of ammonia, with a similar peak in the spectrum as in figure 4.5.

The area under the ammonia peak in the spectrum can be converted to a concentration by using calibration measurements. Calibration curves for a gas chromatograph have been made in the MECS group before[13], which is a linear curve through the origin relating the area under the ammonia peak to a concentration in parts-per-million. Additional calibration measurements were performed on the gas chromatograph, using NH_3 of known concentration in N_2 gas.

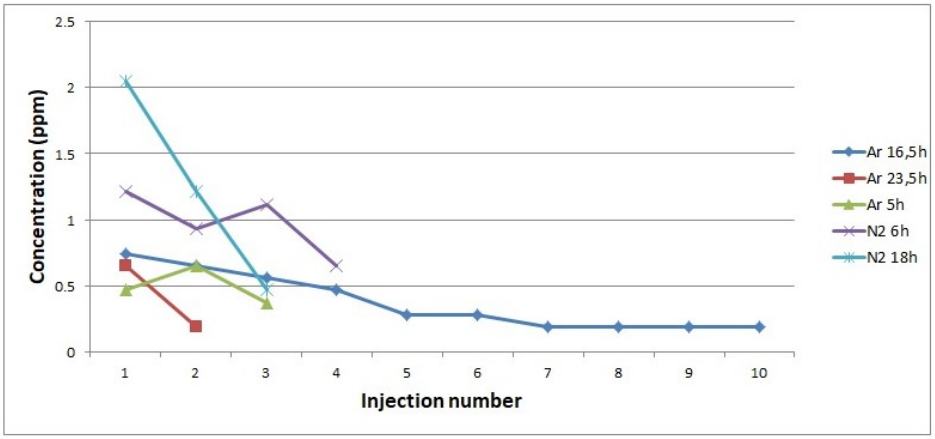

Figure 4.6: Comparison of several gas chromatography measurements after filling the flow cell with either N_2 or Ar gas and leaving the porous iron electrode in contact with the gas for a number of hours. Electrolyte flow through the cell was 0.5 ml/min at all times. After accumulation of ammonia in the cell, the GC measurements were performed using a gas flow which varied between 0.13 and 0.5 ml/min. Ammonia synthesis experiments were performed at a fixed current of 1mA corresponding to a 0.07V potential difference of the working electrode versus the hydrogen reference electrode and a cell voltage of 1.47V.

Figure 4.6 shows the results of several gas chromatography measurements using both N_2 and Ar gas. In general, the concentrations measured after contact with N_2 gas are higher than when Ar gas is used. Also, longer accumulation times lead to more ammonia in the measurements. This indicates that, while there is probably contamination in the measurements, the porous iron electrode may be capable of nitrogen reduction to ammonia. However, the concentrations are very low for a process that takes several hours. For comparison, Ripepi *et al.* reports pure N_2 and Ar feed gas to have less than 150 ppb of ammonia contamination.[24] This is less than the values reported here and the measured NH_3 concentration with N_2 gas in the setup is about one order of magnitude higher. Therefore, the difference in NH_3 concentration between measurements with N_2 and Ar gas cannot be fully explained by differences in the contamination of the feed gas alone. Taking the N_2 measurement after 6 hours of accumulation as an example, a faradaic efficiency was calculated by comparing the amount of NH_3 gas flowing through the gas chromatograph to the amount of charge added during the accumulation time. This resulted in a faradaic efficiency of 0.00027%. Assuming some of the ammonia production is due to nitrogen contamination means this number should be even lower.

5

Discussion

While the results of the gas chromatography experiments show some activity of the porous iron electrode for the reduction of either nitrogen or impurities to ammonia, the amount of ammonia produced is very low. The measurements while cycling the electrode clearly show the iron surface was sufficiently reduced and the potentials applied allow for the formation of ammonia. The cause of the low ammonia yield should therefore be found in other factors. A common explanation in literature for the difficulty of the nitrogen reduction reaction to ammonia is the breaking of the triple bond of the nitrogen molecule. However, the nitrogen permeation experiments done in the MECS group,[5,13] as well as older research by Ertl *et al.* from the 1980s,[34,35] show nitrogen dissociation to be very well possible on a clean reduced catalytic metal surface, even at ambient temperature and pressure. The presence of the catalyst should therefore be sufficient for the cleaving of the nitrogen molecular bond, unless the nitrogen molecules are unable to adsorb on the reduced iron surface. The inability of nitrogen molecules to adsorb on the electrode surface is therefore one way to explain the low ammonia yield.

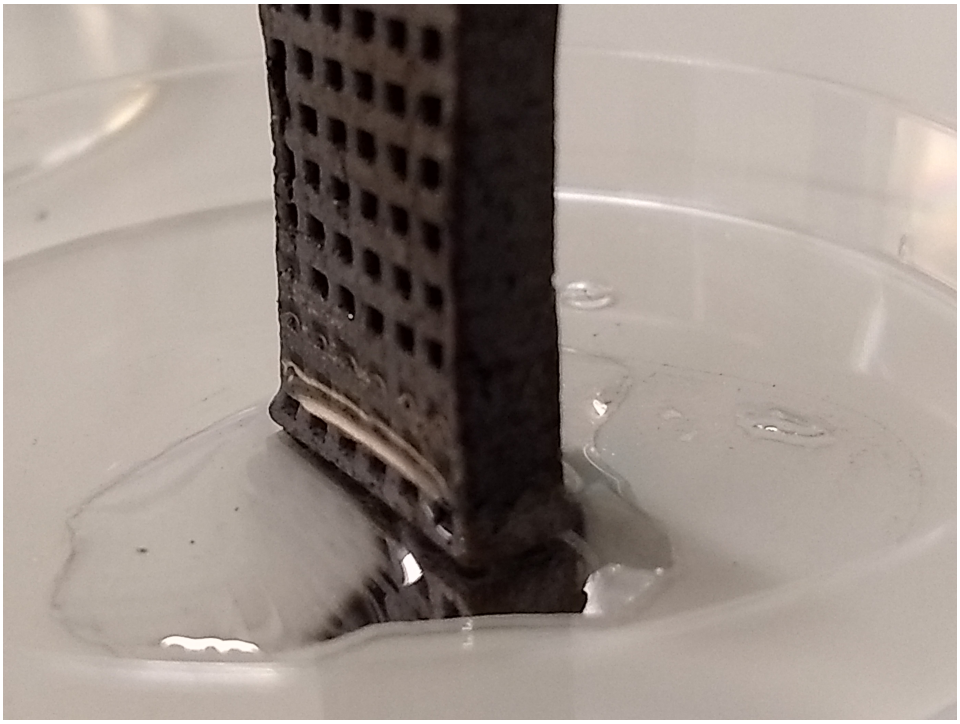

Figure 5.1: Test of the ability of the electrode to absorb electrolyte into its pores. A thin film of electrolyte can be seen on the surface, blocking the bottom three rows of channels of the 3d structure.

One possibility is limited nitrogen dissolution into the electrolyte, which may have blocked nitrogen molecules from reaching the electrode surface. Figure 5.1 shows the porous iron electrode shaped using a mould inside a few drops of electrolyte. A thin film of aqueous electrolyte is clearly visible on the side of the electrode and the three bottom rows of pores are completely wet. The thin film of electrolyte blocks direct access of nitrogen gas to the surface. Therefore, nitrogen needs to dissolve into the thin film of electrolyte before being able to reach the surface. The presence of electrolyte was expected beforehand, since as the hydrogen source, it is desirable for electrolyte to be present in the pores of the material. For this reason, an electrolyte concentration of 1M KOH was used instead of 6M KOH. Combined with the short distance the nitrogen molecule would need to diffuse compared to a fully submerged electrode, it was expected nitrogen would be able to reach the surface easily. This may not have been the case as the large channels also became partly flooded. Figure 5.1 also shows the capillary channels of the 3D electrode are easily filled with electrolyte, which means they do not increase the electrode surface area that is in contact with the gas, as was initially intended.

Another possibility is poisoning of the adsorption sites of nitrogen. The applied potential keeps the iron surface reduced, meaning the formation of oxides or hydroxides is not a concern. The reduction of the iron surface therefore ensures adsorption sites for nitrogen molecules exist. However, if another molecule besides nitrogen can adsorb on these sites, they will block the adsorption of nitrogen. Ertl *et al.* have reported on this as well, noting the competition between adsorption of hydrogen and nitrogen molecules on iron surfaces.[34] One example of this is the hydrogen evolution reaction (HER) competing with the nitrogen reduction reaction, which has been discussed before. However, the HER was suppressed by choosing the optimal potential. Therefore, not all nitrogen adsorption sites are occupied by hydrogen.

However, the lack of HER will not prevent water molecules from adsorbing on the nitrogen adsorption sites. Water strongly adsorbs on Fe surfaces as well: adsorption energies of more than 0.4eV are reported by White *et al.* based on density functional theory (DFT) calculations for several types of Fe surfaces.[36] It should be noted, however, that these calculations are gas phase calculations. For the situation with an electrolyte present one should subtract the heat of evaporation of the electrolyte, since the adsorbed H_2O will rather dissolve in the liquid than evaporate to a gas phase. The heat of evaporation of water is around 40kJ/mol or 0.41eV per molecule, which would be even higher for a KOH solution. Therefore, a water molecule only has a weak tendency to adsorb when a liquid electrolyte is present. However, White *et al.* also report the dissociative water adsorption energy, where water dissociates into adsorbed OH and H after adsorption on a reduced iron surface. This significantly increases the adsorption energy up to 1.8eV depending on the type of iron surface and the surface coverage. Furthermore, the fact that there are much more water molecules present than nitrogen molecules will favor water adsorption over nitrogen. Based on the nitrogen concentration in water as calculated in chapter 2, up to 87000 times more water than nitrogen may be present at the electrode surface. This means the main barrier for nitrogen adsorption and reduction is likely the lack of a clean catalytic surface and not the triple bond of the nitrogen molecule.

Finally, another possible cause for low ammonia yield is a lack of ammonia desorption. Ripepi *et al.* have noted the final desorption of ammonia to be a rate limiting step in nitrogen reduction to ammonia.[13] A lack of desorption of ammonia means the nitrogen adsorption sites remain occupied, blocking further ammonia synthesis. To prevent different experiments building up surface trapped NH_3, the flow cell was often cycled through the battery charge and discharge cycles in between experiments. Any ammonia stuck on the electrode surface will have desorbed as a result of the oxidation and subsequent reduction of the iron it is adsorbed to as well as competition from the HER. According to the Pourbaix diagram of nitrogen in figure 2.4, the slightly positive potentials during the discharge cycle could also oxidise the NH_3 to N_2 and H_2O. Any desorbed NH_3 can still end up as dissolved NH_3 at the positive counter electrode and form NO_x there. Considering no large nitrate or nitrite concentrations were measured and no effect of the electrode cycling on the ammonia content of the gas, it can be concluded a lack of ammonia desorption was not a concern.

6

Conclusion and recommendations

An alternative electrode for electrochemical nitrogen reduction to ammonia was researched. Compared to previous research,[5,13,15,16,24] a porous iron electrode was expected to have an increased catalytic surface area, which would increase ammonia yield. The surface of the porous iron electrode was successfully reduced electrochemically. The electrode was then put inside an electrochemical flow cell on the interface between an aqueous electrolyte and nitrogen gas, to allow for both a hydrogen and a nitrogen source to have easy access to the electrode surface. The competitive hydrogen evolution reaction was suppressed by careful consideration of the applied potential. Keeping the electrode surface reduced electrochemically should have created the right conditions for nitrogen adsorption and reduction. An alkaline electrolyte was used to prioritize ammonia formation in the gas phase, allowing for gas chromatography measurements of the gas flow.

Surprisingly, in gas chromatography measurements of a continuous N_2 gas flow through the cell no ammonia is visible. Only when the gas flow is kept at zero for several hours, trapping gas inside the flow cell and allowing ammonia to accumulate, can any amount of ammonia be measured. This indicates the ammonia yield is very low. Furthermore, verification measurements using argon gas instead of nitrogen also yield some amount of ammonia, albeit even lower amounts. Therefore, at least some of the produced ammonia may be due to contamination by nitrogen containing compounds, despite ion chromatography measurements not detecting these compounds in the electrolyte in significant amounts. Nuclear magnetic resonance spectroscopy measurements have also not detected any ammonia dissolved into the electrolyte. It must therefore be concluded that the porous iron electrode used in this research is not suitable for ammonia synthesis in the experimental setup used.

The low ammonia yield is not caused by failing to break the often reported strong nitrogen molecule triple bond, since past research clearly shows a reduced iron surface is capable of nitrogen dissociation, even at ambient temperature and pressure.[5,13,34,35] The research performed here differs from past research in the abundant presence of water molecules from the aqueous electrolyte. The high wetting of the porous iron electrode must therefore be the cause of the low ammonia yield, resulting from water molecules blocking access of nitrogen to the electrode surface. Either the nitrogen fails to dissolve into a thin film of electrolyte present on the electrode surface or water molecules poison the nitrogen adsorption sites on the electrode surface. This has wider implications for the field of electrochemical ammonia synthesis, since it indicates finding a suitable catalyst for the breaking of the nitrogen triple bond is not the most pressing concern. Instead, the main issue is that catalysts capable of breaking this bond only work when the surface is clean, which contradicts with the use of an aqueous electrolyte.

The flow cell setup used here may only work if barriers to nitrogen reaching the electrode surface are removed. Future research can lower the KOH concentration of the electrolyte even further to 0.1M without changing the electrochemistry. A lower pH can promote dissolution of more nitrogen molecules following Henry's Law, but this may also cause any ammonia produced to prefer dissolving into the electrolyte as well. Another option is to lower the electrode wetting by lowering the electrolyte surface tension through addition of a surfactant to the electrolyte or by adding some hydrophobic material to the electrode. This also makes it easier to increase the electrode surface area through methods like the 3D electrode used in this research. Finally, it is also an option to accept the low ammonia yield of the flow cell setup and instead pass the nitrogen gas through multiple flow cell setups in succession

or through the same cell multiple times. This does require a redesign of the cell setup, but may increase the ammonia yield. In any case, an additional check for contamination by nitrogen containing compounds is desirable. This is commonly done by isotopic labeling experiments, which means $^{15}N_2$ is used as the input gas. Gas chromatography coupled with mass spectrometry can then detect different isotopologues of ammonia and therefore if any ammonia produced is formed through nitrogen dissociation of the input gas or by hydrogenation of other nitrogen containing compounds. Currently these experiments could not be performed because of lack of NH_3 to start with.

Bibliography

(1) European Commission *A Green Deal Industrial Plan for the Net-Zero Age - COMMUNICATION FROM THE COMMISSION TO THE EUROPEAN PARLIAMENT, THE EUROPEAN COUNCIL, THE COUNCIL, THE EUROPEAN ECONOMIC AND SOCIAL COMMITTEE AND THE COMMITTEE OF THE REGIONS*; 2023, https://commission.europa.eu/system/files/2023-02/COM_2023_62_2_EN_ACT_A%20Green%20Deal%20Industrial%20Plan%20for%20the%20Net-Zero%20Age.pdf.

(2) Mulder, F. M. Implications of diurnal and seasonal variations in renewable energy generation for large scale energy storage. *Journal of Renewable and Sustainable Energy* **2014**, *6*, 033105, DOI: 10.1063/1.4874845, https://doi.org/10.1063/1.4874845.

(3) Market Observatory for Energy *Quarterly report on European electricity markets*; European Commission, Q2 2023, https://energy.ec.europa.eu/system/files/2023-12/New_Quarterly_Report_on_European_Electricity_markets_Q2_2023.pdf.

(4) Smil, V. Detonator of the population explosion. *Nature* **1999**, *400*, 415, DOI: 10.1038/22672.

(5) Ripepi, D.; Zaffaroni, R.; Schreuders, H.; Boshuizen, B.; Mulder, F. M. Ammonia Synthesis at Ambient Conditions via Electrochemical Atomic Hydrogen Permeation. *ACS Energy Letters* **2021**, *6*, 3817–3823, DOI: 10.1021/acsenergylett.1c01568.

(6) Xie, H.-Q.; Zheng, X.; Feng, Q.-Y.; Chen, X.-P.; Zou, Z.-H.; Wang, Q.-X.; Tang, J.; Li, Y.; Ling, Y. Single-Step Synthesis of Fe−Fe3O4 Catalyst for Highly Efficient and Selective Electrochemical Nitrogen Reduction. *ChemSusChem* **2022**, *15*, e202200919, DOI: https://doi.org/10.1002/cssc.202200919.

(7) Jiao, F.; Xu, B. Electrochemical Ammonia Synthesis and Ammonia Fuel Cells. *Advanced Materials* **2019**, *31*, 1805173, DOI: https://doi.org/10.1002/adma.201805173.

(8) MacFarlane, D. R.; Cherepanov, P. V.; Choi, J.; Suryanto, B. H.; Hodgetts, R. Y.; Bakker, J. M.; Ferrero Vallana, F. M.; Simonov, A. N. A Roadmap to the Ammonia Economy. *Joule* **2020**, *4*, 1186–1205, DOI: https://doi.org/10.1016/j.joule.2020.04.004.

(9) U.S. Department of Energy *Renewable Energy to Fuels Through Utilization of EnergyDense Liquids (REFUEL) Program Overview*; 2016, https://arpa-e.energy.gov/sites/default/files/documents/files/REFUEL_ProgramOverview.pdf.

(10) Züttel, A.; Remhof, A.; Borgschulte, A.; Friedrichs, O. Hydrogen: the future energy carrier. *Philosophical Transactions of the Royal Society A* **2010**, *368*, 3329–3342, DOI: 10.1098/rsta.2010.0113.

(11) Lan, R.; Irvine, J. T.; Tao, S. Ammonia and related chemicals as potential indirect hydrogen storage materials. *International Journal of Hydrogen Energy* **2012**, *37*, 10th International Conference on Clean Energy 2010, 1482–1494, DOI: https://doi.org/10.1016/j.ijhydene.2011.10.004.

(12) Liu, D.; Zhao, W.; Yuan, Q. Breaking the Linear Relation in the Dissociation of Nitrogen on Iron Surfaces. *ChemPhysChem* **2022**, *23*, e202200147, DOI: https://doi.org/10.1002/cphc.202200147.

(13) Ripepi, D.; Izelaar, B.; van Noordenne, D. D.; Jungbacker, P.; Kolen, M.; Karanth, P.; Cruz, D.; Zeller, P.; Pérez-Dieste, V.; Villar-Garcia, I. J.; Smith, W. A.; Mulder, F. M. In Situ Study of Hydrogen Permeable Electrodes for Electrolytic Ammonia Synthesis Using Near Ambient Pressure XPS. *ACS Catalysis* **2022**, *12*, 13781–13791, DOI: 10.1021/acscatal.2c03609.

(14) Mulder, F. M.; Weninger, B. M. H.; Middelkoop, J.; Ooms, F. G. B.; Schreuders, H. Efficient electricity storage with a battolyser, an integrated Ni–Fe battery and electrolyser. *Energy Environ. Sci.* **2017**, *10*, 756–764, DOI: 10.1039/C6EE02923J.

(15) Zaffaroni, R.; Ripepi, D.; Middelkoop, J.; Mulder, F. M. Gas Chromatographic Method for In Situ Ammonia Quantification at Parts per Billion Levels. *ACS Energy Letters* **2020**, *5*, 3773–3777, DOI: 10.1021/acsenergylett.0c02219.

(16) Ripepi, D.; Zaffaroni, R.; Kolen, M.; Middelkoop, J.; Mulder, F. M. Operando isotope selective ammonia quantification in nitrogen reduction studies via gas chromatography-mass spectrometry. *Sustainable Energy Fuels* **2022**, *6*, 1945–1949, DOI: 10.1039/D2SE00123C.

(17) US Department of Energy Hydrogen Production: Natural Gas Reforming (Accessed on February 1st, 2024), https://www.energy.gov/eere/fuelcells/hydrogen-production-natural-gas-reforming.

(18) The Royal Society *Ammonia: zero-carbon fertiliser, fuel and energy store - POLICY BRIEFING*; 2020, royalsociety.org/green-ammonia.

(19) Appl, M. In *Ullmann's Encyclopedia of Industrial Chemistry*; John Wiley & Sons, Ltd: 2006, DOI: https://doi.org/10.1002/14356007.a02_143.pub2.

(20) Clark, J. The Haber Process (Accessed on January 28th, 2024), https://chem.libretexts.org/Bookshelves/Physical_and_Theoretical_Chemistry_Textbook_Maps/Supplemental_Modules_(Physical_and_Theoretical_Chemistry)/Equilibria/Le_Chateliers_Principle/The_Haber_Process.

(21) Atkins, P.; de Paula, J., *Atkins' Physical Chemistry*, 10th ed.; Oxford University Press: 2014; Chapter 10, pp 398–419.

(22) Guo, Y. et al. Electrochemical Nitrate Production via Nitrogen Oxidation with Atomically Dispersed Fe on N-Doped Carbon Nanosheets. *ACS Nano* **2022**, *16*, 655–663, DOI: 10.1021/acsnano.1c08109.

(23) Dahl, S.; Logadottir, A.; Jacobsen, C. J.; Nørskov, J. K. Electronic factors in catalysis: the volcano curve and the effect of promotion in catalytic ammonia synthesis. *Applied Catalysis A: General* **2001**, *222*, Celebration Issue, 19–29, DOI: https://doi.org/10.1016/S0926-860X(01)00826-2.

(24) Izelaar, B.; Ripepi, D.; van Noordenne, D. D.; Jungbacker, P.; Kortlever, R.; Mulder, F. M. Identification, Quantification, and Elimination of NOx and NH3 Impurities for Aqueous and Li-Mediated Nitrogen Reduction Experiments. *ACS Energy Letters* **2023**, *8*, 3614–3620, DOI: 10.1021/acsenergylett.3c01130.

(25) Sander, R. Compilation of Henry's law constants (version 4.0) for water as solvent. *Atmospheric Chemistry and Physics* **2015**, *15*, 4399–4981, DOI: 10.5194/acp-15-4399-2015.

(26) Kim, J.-H.; Dai, T.-Y.; Yang, M.; Seo, J.-M.; Lee, J. S.; Kweon, D. H.; Lang, X.-Y.; Ihm, K.; Shin, T. J.; Han, G.-F.; Jiang, Q.; Baek, J.-B. Achieving volatile potassium promoted ammonia synthesis via mechanochemistry. *Nature Communications* **2023**, *14*, 2319, DOI: 10.1038/s41467-023-38050-2.

(27) Jain, A.; Ong, S. P.; Hautier, G.; Chen, W.; Richards, W. D.; Dacek, S.; Cholia, S.; Gunter, D.; Skinner, D.; Ceder, G.; Persson, K. A. Commentary: The Materials Project: A materials genome approach to accelerating materials innovation. *APL Materials* **2013**, *1*, 011002, DOI: 10.1063/1.4812323, https://next-gen.materialsproject.org/pourbaix.

(28) Hales, J. M.; Drewes, D. R. Solubility of ammonia in water at low concentrations. *Atmospheric Environment (1967)* **1979**, *13*, 1133–1147, DOI: https://doi.org/10.1016/0004-6981(79)90037-4.

(29) Hodgetts, R. Y.; Du, H.-L.; MacFarlane, D. R.; Simonov, A. N. Electrochemically Induced Generation of Extraneous Nitrite and Ammonia in Organic Electrolyte Solutions During Nitrogen Reduction Experiments. *ChemElectroChem* **2021**, *8*, 1596–1604, DOI: https://doi.org/10.1002/celc.202100251.

(30) Chen, Y.; Liu, H.; Ha, N.; Licht, S.; Gu, S.; Li, W. Revealing nitrogen-containing species in commercial catalysts used for ammonia electrosynthesis. *Nature Catalysis* **2020**, *3*, 1055–1061, DOI: https://doi.org/10.1038/s41929-020-00527-4.

(31) Ishibashi, T.; Himeno, M.; Imaizumi, N.; Maejima, K.; Nakano, S.; Uchida, K.; Yoshida, J.; Nishio, M. NOx Contamination in Laboratory Ware and Effect of Countermeasures. *Nitric Oxide* **2000**, *4*, 516–525, DOI: https://doi.org/10.1006/niox.2000.0302.

(32) Kolen, M.; Smith, W. A.; Mulder, F. M. Accelerating 1H NMR Detection of Aqueous Ammonia. *ACS Omega* **2021**, *6*, 5698–5704, DOI: 10.1021/acsomega.0c06130, https://doi.org/10.1021/acsomega.0c06130.

(33) Fulmer, G. R.; Miller, A. J. M.; Sherden, N. H.; Gottlieb, H. E.; Nudelman, A.; Stoltz, B. M.; Bercaw, J. E.; Goldberg, K. I. NMR Chemical Shifts of Trace Impurities: Common Laboratory Solvents, Organics, and Gases in Deuterated Solvents Relevant to the Organometallic Chemist. *Organometallics* **2010**, *29*, 2176–2179, DOI: 10.1021/om100106e.

(34) Ertl, G.; Huber, M.; Lee, S.; Paál, Z.; Weiss, M. Interactions of nitrogen and hydrogen on iron surfaces. *Applications of Surface Science* **1981**, *8*, 373–386, DOI: https://doi.org/10.1016/0378-5963(81)90092-1.

(35) Ertl, G.; Lee, S.; Weiss, M. Kinetics of nitrogen adsorption on Fe(111). *Surface Science* **1982**, *114*, 515–526, DOI: https://doi.org/10.1016/0039-6028(82)90702-6.

(36) White, J. J.; Hinsch, J. J.; Bennett, W. W.; Wang, Y. Theoretical understanding of water adsorption on stepped iron surfaces. *Applied Surface Science* **2022**, *605*, 154650, DOI: https://doi.org/10.1016/j.apsusc.2022.154650.